nature neuroscience

Silencing of EphA3 through a *cis* interaction with ephrinA5

Ricardo F Carvalho[1], Martin Beutler[2], Katharine J M Marler[1], Bernd Knöll[1,3], Elena Becker-Barroso[1,3], R Heintzmann[2], Tony Ng[2] & Uwe Drescher[1]

EphAs and ephrinAs are expressed in multiple areas of the developing brain in overlapping countergradients, notably in the retina and tectum. Here they are involved in targeting retinal axons to their correct topographic position in the tectum. We have used truncated versions of EphA3, single–amino acid point mutants of ephrinA5 and fluorescence resonance energy transfer technology to uncover a *cis* interaction between EphA3 and ephrinA5 that is independent of the established ligand-binding domain of EphA3. This *cis* interaction abolishes the induction of tyrosine phosphorylation of EphA3 and results in a loss of sensitivity of retinal axons to ephrinAs in *trans*. Our data suggest that formation of this complex transforms the uniform expression of EphAs in the nasal part of the retina into a gradient of functional EphAs and has a key role in controlling retinotectal mapping.

Members of the Eph family of receptor tyrosine kinases and their ephrinA ligands have an instructive role in the development of the retinotectal projection, which serves as a model system for understanding topographic projections[1]. The Eph family consists of the EphA and EphB subfamilies and represents the largest known subfamily of receptor tyrosine kinases[2,3]. In general, EphA receptor tyrosine kinases interact with glycosylphosphatidylinisotol (GPI)-anchored ephrinAs, and EphBs interact with transmembrane ephrinBs, although there are exceptions to this rule (for review, see ref. 4). Ephs and ephrins can function both as receptors and ligands, and understanding this capacity for bidirectional signaling is critical to fully elucidating the physiological roles of the Eph family[5,6]. In the retinotectal projection, temporal axons project onto the anterior tectum and nasal axons onto the posterior tectum, and dorsal and ventral retina are connected to lateral and medial tectum, respectively. With retinal axons initially invading the tectum in a nontopographic fashion (as in chick and mouse) the retinotectal map subsequently develops through topographically specific branching governed by an apparent interplay between uniformly expressed branch-promoting activities and differentially expressed branch-inhibiting activities[7].

EphAs and ephrinAs are thought to be part of a system suppressing topographically unspecific branching[8,9], being expressed in complex countergradients in both the retina and tectum. In sum, EphA receptors have higher expression in the temporal part of the retina than in the nasal part, and ephrinAs are found in the tectum in a posterior→anterior gradient. These differential expression patterns seem to be important for an inhibition of branching posterior to future termination zones[9]. Then, ephrinA 'receptors' are found in a nasal→temporal gradient in the retina, and EphA 'ligands' in an anterior→posterior gradient in the tectum[6] and have been proposed to be involved here in suppressing branching anterior to future termination zones[10]. As a consequence, there is a substantial coexpression of EphAs and ephrinAs on retinal ganglion cell axons. For retinotectal mapping this raises multiple questions: for example, whether EphA receptors expressed on retinal axons interact differently with ephrinAs coexpressed on retinal axons (in *cis*) compared with those ephrinAs expressed in the tectum (in *trans*).

Previous *in vitro* and *in vivo* experiments have provided preliminary evidence for an interplay between coexpressed EphAs and ephrinAs on retinal axons that affects their sensitivity towards ephrinAs presented in *trans*. This has led to the idea that *cis*- and *trans*- presented ephrinAs exert opposing functions on EphA receptors[11]. Thus, overexpression of ephrinAs on temporal axons (in *cis*) resulted in their desensitization in stripe assay experiments, whereas removal of ephrinAs from formerly insensitive nasal axons renders these sensitive towards ephrinAs provided in *trans*[11]. *In vivo*, retrovirally mediated overexpression of ephrinAs on retinal ganglion cells led to a disturbance of the topographic targeting of temporal and nasal axons, indicating a loss of sensitivity towards the repellent ephrinA gradient in the tectum[11]. However, the molecular basis of the interplay between coexpressed EphAs and ephrinAs had not yet been addressed.

Overlapping complementary gradients of EphAs and ephrinAs are not confined to the retinotectal projection; they exist in numerous other regions of the nervous system, such as the cortex and thalamic nuclei (data not shown; see also ref. 12) Furthermore, the coexpression of axon guidance receptors and their ligands, though still poorly understood, is a recurrent theme throughout the nervous system (see refs. 13–17).

[1]Medical Research Council, Centre for Developmental Neurobiology and [2]Randall Division of Cell and Molecular Biophysics, King's College London, New Hunt's House, Guy's Hospital Campus, London SE1 1UL, UK. [3]Present addresses: Institute for Cell Biology, Department of Molecular Biology, University of Tübingen, Auf der Morgenstelle 15, 72076 Tübingen, Germany (B.K.) and The Lancet Neurology, 32 Jamestown Road, London NW1 7BY, UK (E.B.-B.). Correspondence should be addressed to U.D. (uwe.drescher@kcl.ac.uk).

Received 22 December 2005; accepted 27 January 2006; published online 19 February 2006; doi:10.1038/nn1655

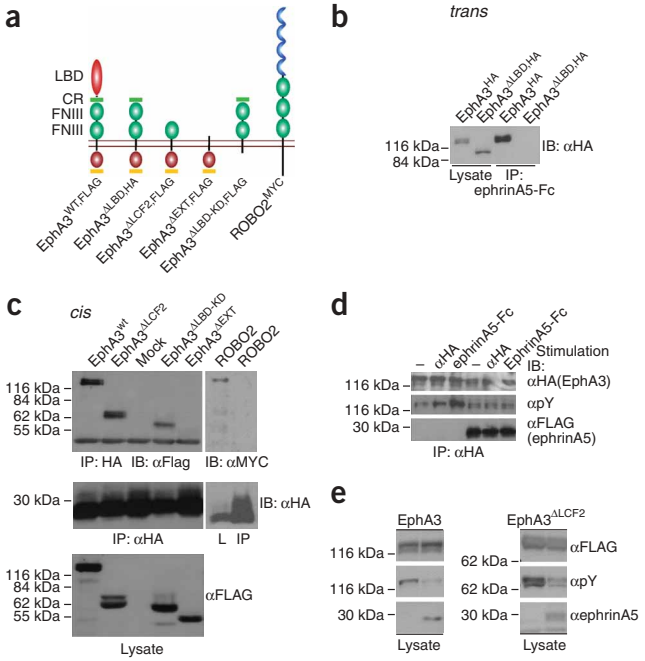

Figure 1 *Cis* interaction between ephrinA5 and EphA3. (**a**) Domain structure of wild-type and mutant EphA3 proteins and of Robo2 (Robo). (**b**) EphrinA5-Fc pull-down from membranes expressing either a full-length HA-tagged EphA3 receptor ($EphA3^{HA}$) or $EphA3^{\Delta LBD,HA}$. The precipitates were subsequently analyzed using an antibody against HA (αHA). These data demonstrate that ephrinA5-Fc binds in *trans* and precipitates $EphA3^{HA}$ but not $EphA3^{\Delta LBD,HA}$. Both EphA3 forms were expressed at similar levels, as shown by analyzing lysates from transfected HEK293 cells. (**c**) HEK293 cells were cotransfected with $ephrinA5^{HA}$ and either $EphA3^{wt,Flag}$, $EphA3^{\Delta LCF2,Flag}$ or $Robo2^{MYC}$. Lysates from these cells were immunoprecipitated using anti-Flag or anti-MYC. $EphA3^{wt,Flag}$ and $EphA3^{\Delta LCF2}$ coimmunoprecipitate with $ephrinA5^{HA}$ but not $EphA3^{\Delta EXT}$ or ROBO (see also **Supplementary Fig. 1**). (**d**) HEK293 cells stably expressing $EphA3^{HA}$ were transfected with either GFP (as control) or $ephrinA5^{Flag}$ and were subsequently treated with 1 μg ml^{-1} unclustered ephrinA5-Fc or 5 μg ml^{-1} anti-HA. Then cell lysates were immunoprecipitated and subjected to western blot analysis. Here stimulation with either ephrinA5-Fc or α-HA antibodies resulted in an increase in tyrosine phosphorylation of $EphA3^{HA}$, but coexpression with $ephrinA5^{Flag}$ abolished this increase. (**e**) HEK293 cells were cotransfected with $ephrinA5^{Flag}$ and either $EphA3^{Flag}$ or $EphA3^{\Delta LCF2,Flag}$ and cell lysates analyzed 2 d later. If expressed alone, both $EphA3^{Flag}$ and $EphA3^{\Delta LCF2,Flag}$ show a high level of tyrosine phosphorylation, but coexpression with $ephrinA5^{Flag}$ led to a strong reduction in tyrosine phosphorylation.

Our results provide evidence for a *cis* interaction between ephrinAs and EphAs outside their canonical ligand binding domain (LBD) that silences EphAs at the level of tyrosine phosphorylation and desensitizes the respective axons for ephrinAs presented in *trans*. On the basis of these results, we propose a model implicating EphA/ephrinA *cis* complexes in the control of retinotectal mapping. This further refines both our understanding of the topographic targeting of retinal growth cone (RGC) axons in the tectum and, more generally, EphA-ephrinA bidirectional signaling.

RESULTS

A *cis* interaction between EphA3 and ephrinA5

The general structure of EphA receptors (**Fig. 1a**) includes an amino-terminal ligand binding domain (LBD), a cysteine-rich domain containing an EGF-like motif (CR), two fibronectin type III (FNIII) domains and a transmembrane domain, followed by a cytoplasmic domain that includes the tyrosine kinase domain, a SAM domain and a PDZ motif[3]. We generated truncated forms of the EphA3 receptor to investigate more closely a possible *cis* interaction between EphAs and ephrinAs outside the LBD: $EphA3^{\Delta LBD,HA}$ is an EphA3 molecule without the LBD; $EphA3^{\Delta LCF2,Flag}$ lacks the LBD, the cysteine-rich domain and the first FNIII domain but retains the membrane-proximal FNIII domain; and $EphA3^{\Delta EXT,Flag}$ lacks the entire extracellular part; whereas $EphA3^{\Delta LBD\text{-}KD,Flag}$ contains the same extracellular part as $EphA3^{\Delta LBD}$ as well as lacking the entire intracellular domain (**Fig. 1a**). All forms were tagged with hemagglutinin (HA) or Flag epitopes to facilitate pull-down experiments and detection in western blot analyses.

After transient expression in HEK293 cells, $EphA3^{wt}$ but not $EphA3^{\Delta LBD}$ was precipitated with ephrinA5-Fc in pull-down experiments using membranes from these cells (**Fig. 1b**). This confirms other findings that show that the LBD is necessary for an interaction between EphAs and ephrinAs in *trans*[18].

In the next step, we coexpressed wild-type or truncated forms of EphA3 together with ephrinA5 to investigate possible *cis* interactions. Under these conditions, $EphA3^{wt}$, as well as the truncated forms $EphA3^{\Delta LCF2}$ and $EphA3^{\Delta LBD\text{-}KD}$, coprecipitated with ephrinA5 (**Fig. 1c**). Similar data were obtained for $EphA3^{\Delta LBD}$ (data not shown). In contrast, we did not observe any interaction between ephrinA5 and the $EphA3^{\Delta EXT}$ truncated receptor, indicating that this interaction depends on the EphA3 membrane-proximal FNIII domain (**Fig. 1a**). To demonstrate the specificity of these interactions, we used in control experiments the platelet-derived growth factor (PDGF) receptor as a divergent receptor tyrosine kinase and the axon guidance receptor ROBO2, which, like EphA3, contains a membrane-proximal FNIII domain. Neither of these molecules coprecipitated with ephrinA5 (**Fig. 1c** and **Supplementary Fig. 1** online).

We then investigated whether EphA3 retains its ligand-binding capacity in *trans* in cells coexpressing EphA3 and ephrinA5, or if it is blocked through the *cis* interaction with ephrinA5 ('masking'; ref. 19, **Supplementary Fig. 2** online). As a measure for this, we used the binding of ephrinA5–alkaline phosphatase (AP) applied in *trans* to cells cotransfected with various ratios of EphA3 and ephrinA5. We found that at a low ratio of ephrinA5 to EphA3, there is a strong binding of ephrinA5-AP to EphA3, indicating the availability of the LBD, whereas at higher ephrinA5/EphA3 ratios, the binding of ephrinA5-AP was correspondingly diminished (**Supplementary Fig. 3** online).

We then investigated the effects of coexpressing EphA3 and ephrinA5 on the tyrosine phosphorylation of EphA3. For this purpose, we established a HEK293 cell line stably expressing $EphA3^{HA}$. Treatment with ephrinA5-Fc induced a strong tyrosine phosphorylation of $EphA3^{HA}$ (**Fig. 1d**). However, prior transfection of ephrinA5 into these cells induced very little tyrosine phosphorylation after incubation with ephrinA5-Fc in *trans* (**Fig. 1d**). We then addressed the question of whether the inhibition of tyrosine phosphorylation could be due to a 'masking' phenomenon (see above and **Supplementary Fig. 2**). We found that this was not the case, as we observed an abolishment of tyrosine phosphorylation after treating cells coexpressing $EphA3^{HA}$ and ephrinA5 with an antibody against the HA tag, which mimics the activation of EphA3 by artificially clustering the receptor (**Fig. 1d**) but does not require the interaction with a 'free' LBD.

Next, we investigated whether the inhibition of tyrosine phosphorylation by coexpressed ephrinAs can be observed also for the truncated EphA3 forms devoid of the LBD (**Fig. 1e**). This seemed likely, as our data have shown that a truncated form of EphA3, $EphA3^{\Delta LCF2}$, which

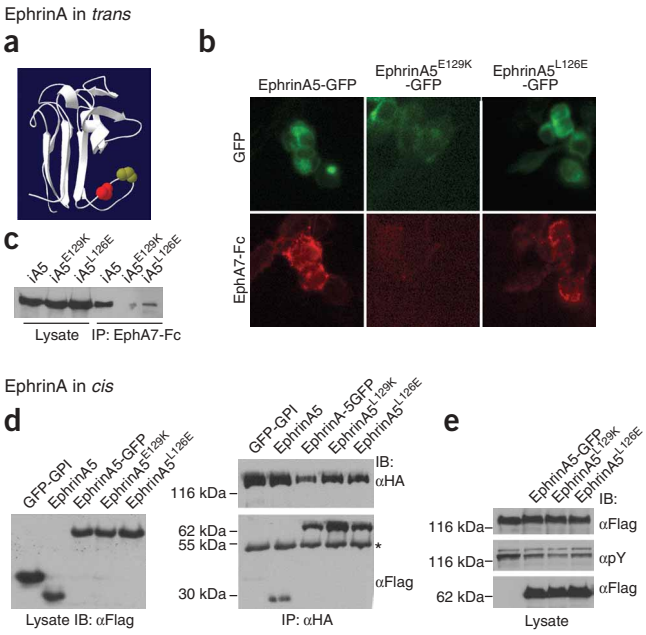

Figure 2 Characterization of single–amino acid changes in ephrinA5-GFP. (**a**) Model of the structure of ephrinB2 (refs. 48,49), which is highly similar to that of ephrinA5, for which structures are available only in its complex with EphB2. An extended G-H loop in the ephrins has a critical role in *trans* ephrin/Eph interactions. Two different single–amino acid mutations were inserted into this loop, the rough positions of which are shown. (**b**) Transfected HEK293 cells with ephrinA5-GFP, ephrinA5-GFP^{E129K} or ephrinA5-GFP^{L126E} analyzed for expression of the fusion proteins and EphA7-Fc binding. Although EphA7-Fc binds strongly to ephrinA5-GFP, there is almost no binding to ephrinA5-GFP^{E129K} and little to ephrinA5-GFP^{L126E}. (**c**) HEK293 cells were transfected with ephrinA5-GFP, ephrinA5-GFP^{E129K} or ephrinA5-GFP^{L126E}. Membranes from these cells were analyzed in a pull-down assay using EphA7-Fc. The data show a strong *trans* interaction between ephrinA5-GFP and EphA7-Fc but little binding of EphA7-Fc to ephrinA5-GFP^{L126E} and even less to ephrinA5-GFP^{E129K}. iA5 represents ephrinA5. (**d**) HEK293 cells were cotransfected with EphA3^{HA}, and either GFP-GPI^{Flag}, ephrinA5^{Flag}, ephrinA5-GFP^{Flag}, ephrinA5-GFP^{E129K,Flag} or ephrinA5-GFP^{L126E,Flag}. Membranes were subjected to immunoprecipitation using anti-HA (right). EphrinA5^{Flag}, ephrinA5-GFP^{Flag} and both ephrinA5 mutants coimmunoprecipitated with EphA3^{HA}, in contrast to GFP^{GPI}, which did not. * marks the position of the immunoglobulin heavy chain derived from the precipitating antibody. (**e**) HEK293 cells were cotransfected with EphA3^{Flag} and either ephrinA5-GFP, ephrinA5-GFP^{E129K} or ephrinA5-GFP^{L126E}. The EphA3 tyrosine phosphorylation seen after transfection of EphA3^{Flag} alone (left) becomes diminished through coexpression with ephrinA5-GFP, ephrinA5-GFP^{E129K} or ephrinA5-GFP^{L126E}.

contains the crucial membrane proximal FNIII domain, was still able to interact with ephrinA5 in *cis* (**Fig. 1c**). Indeed, although transient expression in HEK293 cells of either EphA3^{wt} or EphA3$^{\Delta LCF2}$ alone resulted in their tyrosine phosphorylation (presumably owing to their high level of expression (ref. 20)), cotransfection of ephrinA5 led to an abolishment of this phosphorylation (**Fig. 1e**). These data again show that the blocking of tyrosine phosphorylation involves a *cis* interaction independent of the EphA3-LBD.

EphrinA5 mutants binding to EphA3 in *cis* but not *trans*

In order to further decipher *cis* versus *trans* EphA3/ephrinA5 interactions, we engineered single–amino acid changes into ephrinA5 aimed to disrupt *trans* interactions while retaining *cis* interactions. The basis for the selection of candidate amino acids in ephrinA5 was the crystallographic structure of ephrinB2 in its interaction with its receptor EphB2 in trans[21] and of ephrinA5 with EphB2 (ref. 22). The structure shows an extended, so-called G-H loop of the ephrins juxtaposed with a major groove in EphB2 as the most important interaction domain between EphB2 and the ephrins.

We introduced two different mutations into the G-H loop (**Fig. 2a**). In one mutant, the Glu129 was substituted by lysine (ephrinA5^{E129K}), resulting in a change from a negatively charged amino acid to a positively charged amino acid, and in the other mutant, Leu126 was replaced by glutamate (ephrinA5^{L126E}), exchanging a bulky hydrophobic amino acid for a negatively charged amino acid. Both mutations were designed to disfavor the alignment of the ephrinA5 loop with the EphA3 groove and thus to abolish the EphA3/ephrinA5 *trans* interaction. For a more convenient subsequent functional analysis, in addition to a Flag epitope, these mutants were cloned as enhanced GFP (eGFP) fusion proteins (ephrinA5^{E129K}-GFP and ephrinA5^{L126E}-GFP), taking the monomeric eGFP as a basis to exclude the possibility of any artificial clustering of ephrinA5.

We then analyzed whether these mutations would indeed abolish the *trans* ephrinA5-EphA3 interaction as predicted. For this purpose, we transfected wild-type ephrinA5 (fused to eGFP (ephrinA5^{wt}-GFP)) and the two mutants, ephrinA5^{E129K}-GFP and ephrinA5^{L126E}-GFP, into HEK293 cells and analyzed their ability to bind to EphA receptors in *trans*. This was done first by immunofluorescence using soluble EphA7-Fc as a probe, given that EphA7 binds with high affinity to ephrinA5 (ref. 23). These experiments (**Fig. 2b**) show that EphA7-Fc binds strongly to ephrinA5^{wt}-GFP but only weakly to ephrinA5^{L126E}-GFP and almost undetectably to ephrinA5^{E129K}-GFP. We obtained similar data after expressing these constructs on RGC growth cones (data not shown). Thus, the introduced single–amino acid changes produced the desired effect: an abolishment of EphA3-ephrinA5 interactions in *trans*. We confirmed similar expression levels and membrane localization of wild-type and mutant forms of ephrinA5 on the basis of the coexpressed GFP moiety (**Fig. 2b**). In addition, we verified that coexpression of EphA3 and ephrinA5 ^{E129K} did not block the LBD of EphA3 (**Supplementary Fig. 3**).

We further investigated *trans* ephrinA-EphA interactions by coprecipitation experiments. Using EphA7-Fc, we specifically precipitated ephrinA5^{wt} -GFP from transfected HEK293 cell membranes (**Fig. 2c**); however, we did not detect ephrinA5^{E129K}-GFP at all in EphA7-Fc precipitates and detected only small amounts of ephrinA5^{L126E}-GFP. Experiments performed in parallel showed that all three proteins were expressed in HEK293 cells at similar levels (**Fig. 2c**). Thus, both immunofluorescence and coprecipitation experiments indicated that the ephrinA5^{E129K} mutation disrupted the *trans* EphA/ephrinA interactions more strongly than the ephrinA5^{L126E} mutation.

Finally, we determined the dissociation constants between EphA and ephrinA5^{wt} or ephrinA5^{E129K} on the basis of a Scatchard analysis[24]. As expected, ephrinA5^{wt} and EphA3-AP interact with high affinity (k_D of 4.18 nM; **Supplementary Fig. 4** online), whereas probing ephrinA5^{E129K}–expressing cells with EphA3-AP did not lead to a saturable binding, indicating a nonspecific interaction between these two molecules (**Supplementary Fig. 4**).

In the next step, we investigated whether the mutations introduced have left the *cis* interaction between EphA3 and ephrinA5 intact. We coexpressed EphA3^{HA} in HEK293 cells together with ephrinA5^{wt}, ephrinA5^{E129K}, ephrinA5^{L126E} or GFP^{GPI}, an eGFP molecule attached to the GPI anchor of ephrinA5, serving here as a control (**Fig. 2d**). Pull-down experiments using an antibody against HA showed that ephrinA5^{wt} and both mutants, but not GFP^{GPI}, coprecipitated with EphA3,

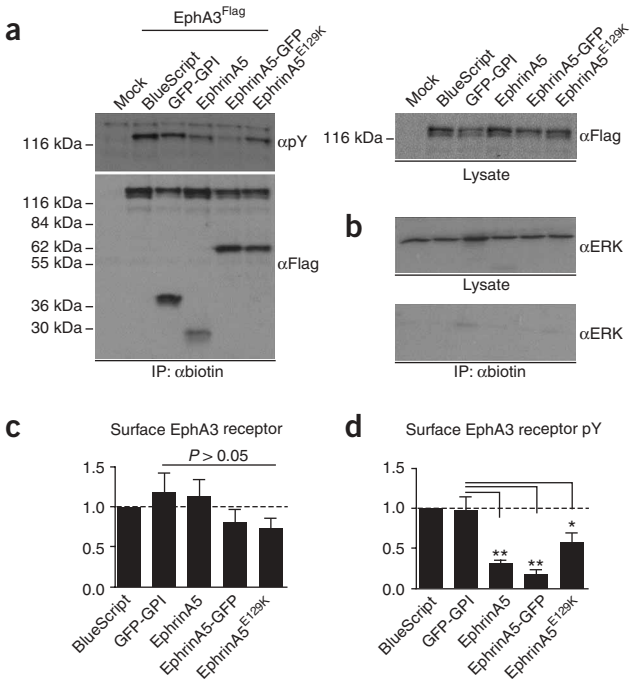

Figure 3 Control of EphA3 tyrosine phosphorylation by coexpressed ephrinAs occurs at the membrane. HEK293 cells were transfected with constructs expressing EphA3^{Flag} and either GFP^{GPI}, ephrinA5, ephrinA5^{wt}-GFP or ephrinA5^{E129K}-GFP. Membrane proteins were purified by labeling the cells with biotin, followed by streptavidin-Sepharose precipitation. (**a**) The tyrosine phosphorylation of the EphA3 receptor in the membrane fraction is downregulated when coexpressed with ephrinA5, ephrinA5^{wt}-GFP or ephrinA5-GFP^{E129K}. (**b**) The location of the intracellular ERK1/2 was used to monitor the enrichment for membrane proteins. (**c**,**d**) Quantification of seven independently performed biotinylation experiments. The intensity of bands from cells transfected with EphA3 and control DNA (BlueScript) was set to 1. (**c**) Fraction of surface receptor versus total receptor compared with the control situation. None of the conditions showed a statistically significant difference from the control. (**d**) Quantification of tyrosine phosphorylation of the EphA3 receptor in the membrane fraction compared with controls and normalization to the amount of membrane receptor in the different conditions. Transfection of GFP^{GPI} did not change the level of EphA3 receptor phosphorylation (0.97 ± 0.17), whereas transfection of ephrinA5 (0.31 ± 0.05), ephrinA5^{wt}-GFP (0.19 ± 0.06) and ephrinA5-GFP^{E129K} (0.56 ± 0.12) resulted in a reduction in its tyrosine phosphorylation. Statistical analysis was performed with GraphPad Prism using one way ANOVA with Dunnett's post test. * $P < 0.05$; ** $P < 0.01$. Bars indicate s.e.m.

indicating that the mutations introduced did not affect the ability of these proteins to interact with EphA3 in *cis*.

Subsequently, we analyzed the tyrosine phosphorylation of EphA3 after coexpression with the different ephrinA5 forms. Here again, ephrinA5^{wt}, as well as both mutant ephrinA5s, led to a reduced tyrosine phosphorylation of the EphA3 receptor (**Fig. 2e**).

In sum, the ephrinA5 mutants retain their capacity to interact with EphA3 in *cis*. The mutants have lost the ability to interact with EphA via the LBD and do not interact with EphA3 in *trans* (**Supplementary Fig. 2**). They thus represent suitable tools for a functional dissection of *cis* and *trans* Eph-ephrin interactions.

EphA/ephrinA interaction at the plasma membrane

To investigate whether the downregulation of EphA phosphorylation occurs at the plasma membrane or if it might be related to other factors such as ligand-induced receptor endocytosis[25,26] or reduced surface localization, we cotransfected EphA3 together with either GFP^{GPI}, ephrinA5, ephrinA5^{wt}-GFP or ephrinA5^{E129K}-GFP into HEK293 cells and isolated the plasma membrane fraction using a protocol including the biotinylation of surface proteins (**Fig. 3**, ref. 27). We found that, compared with control GFP^{GPI} (0.97 ± 0.17), both ephrinA5 (0.31 ± 0.05) and ephrinA5^{wt}-GFP (0.19 ± 0.06) induced a reduction in membrane-bound EphA3 receptor phosphorylation (**Figs. 3a**,**d**). We observed a similar, although slightly less pronounced, reduction (0.56 ± 0.12) for the *trans* interaction–defective mutant ephrinA5^{E129K}-GFP. Coexpression of these different proteins did not change the amount of EphA receptor present on the plasma membrane (**Fig. 3c**). We found only traces of tyrosine phosphorylation of EphA3 receptors outside the plasma membrane fraction compared with the tyrosine phosphorylation of the membrane fractions (data not shown).

EphAs and ephrinAs are uniformly distributed on growth cones

We analyzed the distribution of fluorescent EphA and ephrinA fusion proteins (EphA3-YFP and ephrinA5-CFP) on chick RGC axons and growth cones by live cell imaging (**Fig. 4**). The use of these fusion proteins avoided problems associated with other types of analyses such as antibody staining, which seem to be associated with artificial clustering of proteins owing to antibody-induced cross-linking occurring even after paraformaldehyde fixation (data not shown).

Expression of these fluorescent fusion proteins led to a uniform distribution of both molecules on retinal growth cones, including their filopodia (**Fig. 4a**,**b**, right). Although we observed an occasional spot(s) in growth cone and axon shaft (**Fig. 4c**), live cell imaging showed trafficking of these spots up and down the axon shaft, suggesting that they represent transport vesicles containing EphAs or ephrinAs (data not shown). Notably, we also observed a uniform distribution of ephrinA5-CFP and EphA3-YFP when both molecules were coexpressed (**Fig. 4c**). Thus, within the limits of conventional light microscopy, it may be said that both molecules are colocalized on retinal growth cones.

FRET analysis uncovers EphA3/ephrinA5 complex formation

To study the molecular interaction of EphAs and ephrinAs at a still higher resolution, we investigated fluorescence resonance energy transfer (FRET) between EphA3-YFP and ephrinA5-CFP. The efficiency of FRET is strongly dependent on the distance between donor (CFP) and acceptor (YFP) molecules, it requires a mutual distance of fluorophores in the range of 1 nm to 10 nm[28]. This distance dependency makes FRET an important method for investigating the proximity of proteins. We found that interactions on retinal growth cones between EphA3-YFP and ephrinA5-CFP as well as EphA3-YFP and ephrinA5^{E129K} -CFP resulted in FRET, whereas EphA3-YFP and Transferrin receptor-CFP (TfR-CFP) did not (**Fig. 4d**, **Supplementary Fig. 4**). We observed a clear increase in donor intensity after acceptor photobleaching in the growth cone of retinal ganglion cell axons (marked within the representative cell images in **Supplementary Fig. 5** online). We did not observe such donor recovery in EphA3-YFP and TfR-CFP-transfected cells. We chose TfR as a control, as this molecule is used routinely in protein/lipid biochemistry as a membrane protein not residing within detergent resistant membranes (for example, see ref. 29). As EphAs have been reported to be associated with such membrane subdomains[30,31], the use of TfR in these FRET experiments excludes the possibility that these molecules come by chance into close proximity because of their tendency to associate with a particular lipid environment.

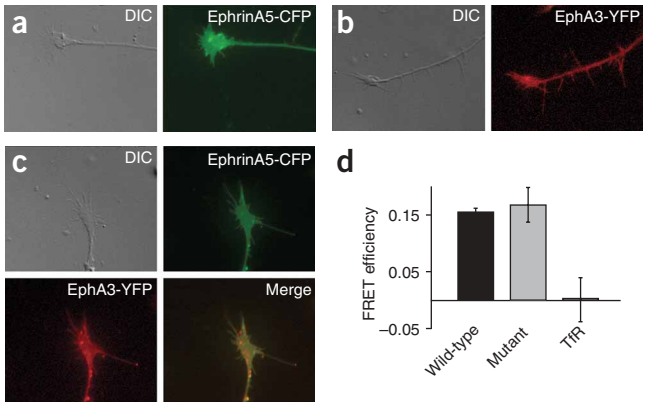

Figure 4 Expression pattern and FRET analysis of ephrinA5-CFP and EphA3-YFP on retinal ganglion cells. (**a**,**b**) Microscopic analysis using a 100× objective showed that electroporated ephrinA5-CFP (**a**, right) and EphA3-YFP (**b**, right) are uniformly distributed on growth cones. Corresponding DIC pictures are shown in **a** (left) and **b** (left). (**c**) Coexpression of ephrinA5-CFP and EphA3-YFP led again to a uniform distribution of both molecules (upper right, lower left) and an extensive colocalization (lower right). (**d**) Mean FRET efficiencies (relative donor increase after acceptor photobleaching) and variances (error bars) for three different types of coexpression: wild-type: EphA3-YFP and ephrinA5-CFP; mutant: EphA3-YFP and ephrinA5^{E129K}-CFP; TfR: EphA3-YFP and TfR-CFP; number of measured cells: $n = 19$ (wild-type), $n = 20$ (mutant and TfR). See also **Supplementary Figure 5**.

In sum, our FRET data demonstrate the existence of EphA3/ephrinA5 complexes on retinal ganglion cell growth cones in *cis*. These interactions are LBD-independent and thus support other biochemical data such as the coimmunoprecipitation of EphA3 and ephrinA5.

Retinal axons lose sensitivity by *cis*-interacting ephrinAs

We then used the growth cone collapse assay to functionally investigate EphA/ephrinA *cis* and *trans* interactions (**Fig. 5**), using ephrinA5^{E129K}-GFP in particular, which showed the strongest abolishment of the LBD-dependent interaction with EphA3 (**Fig. 2b**), while retaining its LBD-independent *cis* interaction with EphA3 (**Fig. 2d**).

We electroporated single cells from chick embryonic day 6 (E6)–E7 temporal retina with corresponding eGFP-tagged constructs and plated them on laminin-coated dishes. After 2 d in culture, we used fluorescence microscopy to identify successfully electroporated RGC axons. We routinely obtained electroporation efficiencies between 20% and 30%; nonelectroporated axons were used as internal negative controls. Growth cone morphology and growth rate of temporal RGC axons apparently were not affected by expression of these proteins, such that for example ephrinA5-GFP expressing axons or growth cones could be discriminated from nonelectroporated ones only by fluorescence microscopy. Expression of ephrinA5^{E129K}-GFP and of ephrinA5^{wt}-GFP in retinal RGCs led to a uniform fluorescence of growth cones (**Fig. 5**), indicating a proper processing and transport of these molecules into retinal growth cones.

We then analyzed RGC axons in the growth cone collapse assay by live cell imaging using a computer-controlled scanning stage, enabling a simultaneous analysis of multiple growth cones in parallel. We performed time-lapse analysis for at least 30 min before and 50 min after bath application of 1 μg ml^{-1} unclustered ephrinA5-Fc (**Fig. 5**; see Methods). Only those growth cones that showed a clear advancement in the initial 30 min were selected for further analysis. Evaluation of these experiments showed that expression of ephrinA5^{E129K}-GFP in *cis* led to a reduced sensitivity towards ephrinA5-Fc in *trans* when compared with axons expressing a GPI-anchored control protein

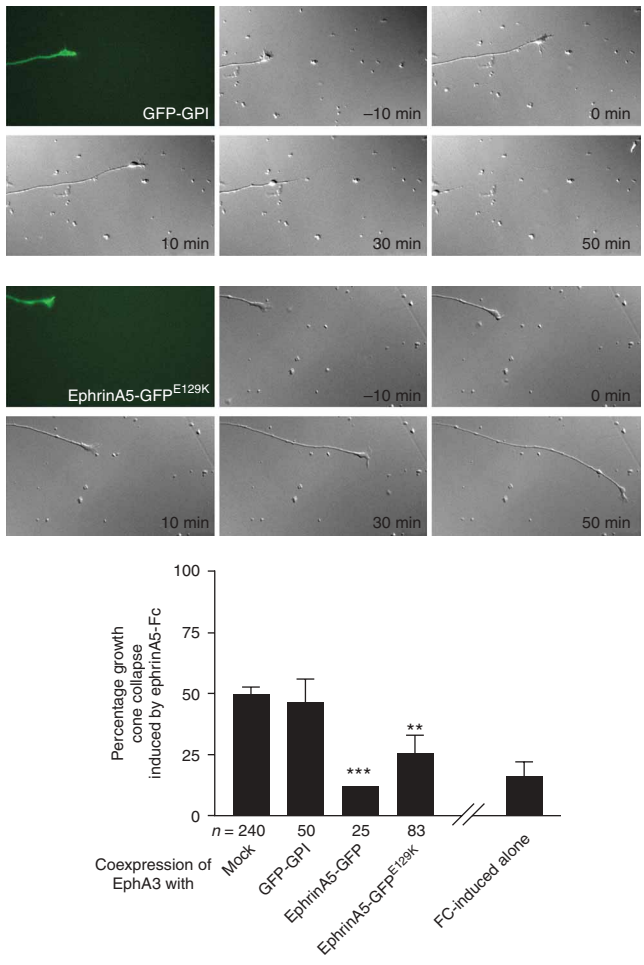

Figure 5 Expression of ephrinA5^{E129K} abolishes sensitivity of temporal retinal axons for ephrinA5 applied in *trans*. After electroporation, cells were plated on laminin-coated dishes. Two days later, the growth cone collapse assay was performed by bath application of 1 μg ml^{-1} unclustered ephrinA5-Fc; this was determined to be the concentration at which about 50% of the growth cones in the control (electroporation of GFP^{GPI}) showed a collapse response. Upper two rows of images show behavior of a temporal growth cone expressing GFP^{GPI}. Before adding ephrinA5-Fc, the growth cone could be seen migrating forward. Roughly 10 min after addition of ephrinA5-Fc, the growth cone collapsed, and later the axon shaft retracted completely. Lower two rows of images show behavior of a temporal growth cone expressing ephrinA5^{E129K}-GFP. Throughout the entire observation period, the axon appeared healthy and migrated further on. Bar graph at bottom shows quantification of growth cone collapse rates. Growth cones from nonelectroporated temporal axons showed a collapse response of 49.97% ± 2.93%; those from GFP^{GPI} electroporated temporal axons, 46.14% ± 9.94%. Temporal axons expressing ephrinA5-GFP or ephrinA5^{E129K}-GFP showed growth cone collapse responses of 12.02% ± 0.47% and 25.74% ± 7.69%, respectively. Results (mean ± s.d.) are from at least four independent experiments for each construct. Application of 1 μg ml^{-1} unclustered Fc resulted in a collapse response of 16% of temporal growth cones. Statistical analysis was performed with GraphPad Prism using the unpaired *t*-test (two-tailed). ** $P < 0.005$; *** $P < 0.001$.

(GFP^{GPI}) or when compared with nontransfected axons (**Fig. 5**). For these latter conditions (serving as controls), we observed a growth cone collapse rate of about 50%, whereas ephrinA5^{E129K}-GFP expression resulted in reduction in the collapse rate to 25% and, in case of ephrinA5^{wt}-GFP, to only 12%.

This loss in sensitivity to ephrinA5-Fc correlates well with the biochemical characterization of ephrinA-EphA interactions, which have shown that coexpression of these molecules resulted in a decrease in tyrosine phosphorylation and thus a silencing of EphA3 function (**Fig. 2**). Notably, the reduction in sensitivity exerted by ephrinA5^{E129K}-GFP was not as pronounced as that of ephrinA5^{wt}-GFP. This observation correlates with the observed decrease in tyrosine phosphorylation of the EphA receptor in the membrane fraction (**Fig. 3a,d**) and might relate to the fact that ephrinA5^{wt} interacts with EphA3 both in a LBD-dependent and a LBD-independent way, whereas ephrinA5^{E129K}-GFP binds to EphA3 only via the LBD-independent *cis* interaction (**Supplementary Fig. 2**).

DISCUSSION

Previous *in vitro* and *in vivo* experiments have shown that modulation of ephrinA expression on retinal ganglion cell axons coexpressing EphA/ephrinA leads to a change in their sensitivity towards externally applied ephrinAs[11]; however, the underlying molecular mechanism had remained unknown.

We have identified and characterized a new type of interaction between EphAs and ephrinAs, independent of the established ligand-binding domain (LBD), that seems to account for this regulatory mechanism at least partially. Formation of the *cis* Eph/ephrin complex leads to an abolishment of the tyrosine phosphorylation of EphA3 and therefore its inactivation, resulting in a loss of sensitivity towards ephrinAs applied in *trans*.

Two types of EphA/ephrinA *cis* interaction

To further characterize this new type of *cis* interaction, we have generated mutants of ephrinA5 with single–amino acid changes. These mutants no longer bind to the amino-terminal LBD of EphAs, but still interact with EphAs via a non-LBD interface (**Figs. 2** and **Supplementary Fig. 2**), as shown by coimmunoprecipitations and FRET on retinal growth cones. The ephrinA mutant ephrinA5^{E129K} was found to abolish the tyrosine phosphorylation of EphA3, and its expression on temporal retinal axons resulted in a desensitization of these axons towards externally ephrinAs applied in *trans*, as shown in the growth cone collapse assay (**Fig. 5**). A comparison of the decrease in growth cone collapse rate of temporal retinal axons caused by the expression of ephrinA5^{wt}-GFP to that of ephrinA5^{E129K}-GFP indicates that both LBD-dependent and LBD-independent *cis* interactions contribute to the silencing of EphA receptors (**Fig. 5** and **Supplementary Fig. 2**).

'Masking' (that is, LBD-dependent Eph/ephrin *cis* and *trans* interactions) and a reduction in tyrosine phosphorylation have been observed in another study[32] after coexpression of EphAs and ephrinAs in HEK293 cells. A *cis* interaction outside of the LBD, however, was not explored in that study. Nevertheless, those results are in concurrence with our data, which indicate the coexistence of both types of *cis* interactions in regulating EphA function.

Another study in NIH3T3 cells also demonstrated that coexpressed ephrinA5 could prevent the activation of EphA3 by bath application of ephrinA5-Fc. Notably, removal of ephrinA5 by treating the cells with phosphatidyl-inositol specific phospholipase C (PI-PIC) was sufficient to rescue the EphA3 receptor sensitivity to activation by ephrinA5-Fc, indicating a cell surface–associated process[33]. Similarly, the tyrosine phosphorylation of EphBs in cells coexpressing ephrinB and EphB was found to be strongly reduced when compared with that of EphB-expressing cells treated with ephrinB-expressing cells[34]. Here also, application of ephrinB-Fc could not induce the tyrosine phosphorylation of EphB. As cells coexpressing ephrinB and EphB form aggregates, as do cells expressing ephrinBs and EphBs separately[34], it seems that in this context, LBD-independent *cis* interactions have a prominent role, and 'masking' does not seem to be involved at all. Similar adhesions have been observed in other cases of coexpression of Ephs and ephrins[35,36].

In contrast, another study performed in chick motor neurons[37] suggests that EphAs and ephrinAs are localized entirely to different membrane domains and signal independently, with EphAs directing growth cone collapse and retraction and ephrinAs signaling motor axon growth and attraction. Also, overexpression of ephrinA5 on EphA4-expressing motor neurons did not modify the growth cone collapse induced by ephrinA1-Fc[37]. Although some of the conclusions of that study seem not to be compatible with the above-mentioned data and our own results, the divergences might be due to differences between motor neurons and retinal ganglion cells.

The mechanism(s) of EphA silencing

What molecular mechanisms could account for the decrease in EphA3 tyrosine phosphorylation? We have shown here that both EphA3 and ephrinA5 must be membrane bound for this *cis* interaction to occur and that the membrane-proximal FNIII domain of EphA3 is critical for this interaction (**Figs. 1** and **2**). Thus, a particular membrane lipid environment might stabilize these EphA/ephrinA interactions and bring these molecules into an optimal configuration, stoichiometry or both. At present, we cannot exclude that the *cis* Eph-ephrin interaction involves additional binding partners; however, FRET observed between the two fluorophores (CFP and YFP, $R_0 = 4.87$ nm; ref. 28) requires a separation of these molecules of no more than 7.3 nm and therefore argues against this possibility (**Fig. 4** and **Supplementary Fig. 5**).

EphrinAs are localized to a special type of lipid raft (a membrane subdomain with a high local concentration of molecules involved in signaling[38]). Owing to the *cis* interaction shown here, ephrinAs might drag EphAs into this particular kind of lipid environment. It is conceivable that in this way, EphAs and some tyrosine phosphatases residing in rafts are brought together, resulting in a dephosphorylation and silencing of EphAs. Ligand-dependent shifts in membrane localization and changes in signaling have been observed previously (for example, the interaction of the receptor tyrosine kinase c-Ret with its ligand GDNF/GFRα1; ref. 39). Another possibility would be that ephrinAs antagonize by sterical interference the clustering and tyrosine phosphorylation of EphAs, which is necessary for their activation[40]. Coexpressed, *cis*-interacting ephrinAs might be involved in terminating or limiting this step.

Notably, the downregulation of EphA receptor tyrosine phosphorylation through *cis* ephrinA interaction occurs at the plasma membrane (**Fig. 3**). As the *trans* activation of EphA receptors leads to the endocytosis of phosphorylated receptor[25,26], this observation further juxtaposes the contrary effects of *cis* and *trans* Eph-ephrin interactions.

Coexpression of EphA and ephrinA in retinotectal mapping

Quantitative *in situ* hybridizations have shown the precise shape of the nasotemporal gradient of EphA mRNA expression in the RGC layer[41] (**Supplementary Fig. 2**). These results have shown that the summed expression of all EphAs in the nasal retina is almost uniform, in

particular as the gradients of EphA5 and EphA6 are mostly confined to temporal retina, and the more strongly expressed EphA4 was not found in a gradient in nasal (or temporal) retina[41].

Recently it has been shown that even very shallow gradients of guidance information can be read by growth cones[42]. However, we propose a prominent role for *cis* interactions of ephrinAs in providing guidance information to nasal retinal axons (see also refs. 8,10,43). Our data suggest a model in which the nasal→temporal gradient of ephrinA expression in the retina transforms the uniform ΣEphA expression in the nasal retina into a gradient of silenced EphA receptors, generating a gradient of the remaining functional (that is, signaling-competent) EphA receptors (**Supplementary Fig. 2**). In this way, a continuous functional EphA gradient would be generated throughout the retina, which is a necessary component for a proper retinotectal mapping.

We propose that on retinal axons there is an equilibrium between EphAs, ephrinAs and ephrinA/EphA complexes. Thus, both EphAs and ephrinAs exert a function as guidance receptors on nasal axons, as indicated, for example, by results from stripe assay experiments, in which nasal axons are repelled from growing on lanes containing either ephrinA5 (see ref. 44) or EphAs[8]. Moreover, some tyrosine phosphorylation of EphA4 has been detected in the retina, which is stronger in nasal than temporal retina, thus correlating with the graded expression of ephrinAs[11,45]. Given the uniform expression of EphA4, this suggests that some, but not all, unbound EphA4 is tyrosine phosphorylated, presumably owing to *trans* activation of ephrinAs (compare ref. 41).

Altogether, our work suggests an additional mechanism for the involvement of ephrinAs and EphAs in retinotectal mapping: the transformation of a uniform retinal EphA distribution into a gradient of functional EphA, using the ephrinA countergradient (**Supplementary Fig. 2**). On the basis of this concept, one might predict that a similar regulation occurs also for temporal axons: that is, a transformation of mostly uniform retinal ephrinA expression into a functional gradient using an EphA countergradient.

METHODS

Cell culture and transfection. Human embryonic kidney 293 (HEK293) cells were grown in Dulbecco's Modified Eagle Medium (DMEM) with 10% fetal calf serum (FCS) and transfected using the standard calcium phosphate method. Stable cells lines were kept in DMEM/10% FCS supplemented with 750 μg ml^{-1} G418. Cells were stimulated for 30 min with 1 μg ml^{-1} nonclustered ephrinA5-Fc or 5 μl ml^{-1} antibody against HA (Covance).

Generation of DNA constructs: introduction of point mutations in ephrinA5. Two mutations in ephrinA5 were chosen to abolish the *trans* interaction between ephrinA5 and EphAs. In ephrinA5^{E129K}, Glu129 is replaced by lysine, and in ephrinA5^{L125E}, Leu125 by glutamate. These mutations were generated by overlap extension PCR using mouse ephrinA5 as template. Resulting *Hin*dIII/*Xba*I fragments were cloned into the p3xFlag-CMV9 expression vector (Sigma), into which monomeric eGFP was cloned subsequently as a *Hin*dIII PCR fragment, resulting in a construct containing the CMV promoter–signal peptide–Flag-eGFP-ephrinA5^{mut}. The inserts were reexamined by sequencing. For expression in neuronal cells, a PCR-generated *Xho*I/*Eco*RI fragment was inserted into the expression vector pCAβ, in which expression of the insert is under control of the chick β-actin promoter.

Cloning of transferrin receptor-CFP (TfR-CFP). Reverse transcription PCR (RT-PCR) was used to amplify the coding region of TfR from E8 chick retina using the oligonucleotides 5′-ATGGATCATGCCAGAGCAGCATTGTCT-3′ and 5′-GTGTCTAGAATTCATTGTCAGTTTCCCAG-3′, and it was cloned using *Not*I-*Bam*HI restriction sites into the BlueScript vector (Stratagene). From here it was cut out and cloned via *Bam*HI-*Xho*I restriction sites into the expression vector pCAβ containing a sequence coding for CFP downstream of TfR. Because TfR is a transmembrane type II protein, CFP will be on the outside of the cell[46]. Uniform expression of this construct on retinal growth cones was verified by fluorescence microscopy.

Generation of truncated versions of EphA3. Truncated versions of EphA3 were generated by cloning subfragments of mouse EphA3, obtained by PCR, in conjunction with cloned EphA3 subfragments into the MCS of p3xFlag-CMV9 (Sigma), which contains a signal peptide followed by three Flag tags. EphA3^{wt,Flag} contains EphA3 sequences immediately 3′ to the signal peptide starting with the amino acid sequence LSPQP, whereas EphA3$^{\Delta LCF2,Flag}$ starts with PSPVM, and EphA3$^{\Delta ext}$ starts with TNSRK. EphA3^{wt,HA} and EphA3$^{\Delta LBD,HA}$ are based on a pCl Neo expression vector containing a CMV promoter and corresponding mouse EphA3 fragments, into which an *Asc*I site was cloned immediately 3′ to the signal peptide. DNA sequences coding for an HA epitope were introduced by oligonucleotides via *Asc*I sites. EphA3$^{\Delta LBD,HA}$ starts with the amino acid sequence CVALVS. DNA derived from PCR fragments was subsequently sequenced.

Pull-down experiments. Cells were washed with cold phosphate-buffered saline (PBS), collected in lysis buffer (50 mM Tris pH 7.5, 150 mM NaCl, 1% Triton, 10% glycerol, 1 mM phenylmethylsulfonylfluoride (PMSF), 1 mM sodium vanadate, 1 mM sodium pyrophosphate, 1 mM glycerophosphate, 1 mM sodium fluoride and protease cocktail inhibitor (Boehringer)) and were incubated on ice for 15 min. Lysates were cleared by centrifugation (15 min, 13,000*g*) and incubated overnight with 5 μg ml^{-1} anti-HA (Covance), 2 μg ml^{-1} EphA7-Fc (R&D), 1 μg ml^{-1} ephrinA5-Fc (R&D) or 5 μg ml^{-1} anti-Flag (Sigma). For analysis of the lysate, 10% of the volume of lysis buffer was removed before adding antibodies. Lysates were subsequently incubated with proteinG or proteinA agarose, washed four times with lysis buffer and resuspended in sample buffer. Standard protocols were used to perform the western blot analyses.

Biotinylation of membrane proteins. Thirty-six hours after transfection, cells were incubated for 10 min at 4 °C to abolish endocytosis. Cells were washed twice with cold PBS and incubated with 1 mg ml^{-1} of NHS-SS–biotin in PBS (pH 8.0) at 4 °C for 30 min, followed by two washes with cold PBS and incubation in quenching buffer (100 mM glycine in PBS) for 15 min at 4 °C. Cells were then washed twice with PBS and harvested in 1% Triton lysis buffer. After 20 min incubation at 4 °C, samples were centrifuged for 15 min at 13,000*g*. The supernatant was then incubated with 50 μl of a 50% slurry of streptavidin-Sepharose beads for 2 h or overnight at 4 °C, followed by four washes with 1 ml lysis buffer each. Then beads were pelleted by centrifugation, the supernatant removed and 40 μl of 2× sample buffer added. Standard protocols were used to perform the western blot analyses.

Single cell retinal explants cultures and electroporation. The nasal or temporal thirds of two of retinas from E7 chick embryos were incubated for 8 min at 37 °C in 500 μl of Worthington trypsin. Trypsinization was stopped by adding 500 μl of 10% FCS in DMEM, and the tissue was homogenized using a Pasteur pipette. Then cells were pelleted by centrifugation (2 min at 2,000*g*) and resuspended in 100 μl of nucleoelectroporation solution (Amaxa) containing 5 μg DNA (GFP^{GPI}, ephrinA5^{wt}-GFP, ephrinA5^{E129K}-GFP, ephrinA5-CFP or EphA3-YFP). Subsequently, cells were electroporated with the Amaxa Nucleofector (G-13 program), diluted in 900 μl of 10% FCS in DMEM and plated on glass plates precoated with 10 μg ml^{-1} poly-L-lysine and 20 μg ml^{-1} laminin. RGCs were grown for 24 h in F12 medium with 0.4% methylcellulose, followed by another 24 h in F12 medium without methylcellulose, and they were subsequently analyzed in the growth cone collapse assay. Axons from retinal ganglion cells could be easily identified by their very long axons.

Growth cone collapse assay. The growth cone collapse assay was performed as described previously[47], using a Zeiss M200 microscope with computer-controlled scanning stage and environmental chamber, kept at 37 °C (5% CO_2). Dishes containing single RGCs were transferred to the chamber at least 30 min before the start of time lapse. Then growth cones were subjected to time-lapse analysis for at least 80 min with frames taken every 5 min. Thirty min after the

start of recording, nonclustered ephrinA5-Fc or Fc protein was added to the medium.

Immunocytochemistry. Twenty four to 36 h after transfection, cells were transferred for 10 min to 4 °C to stop protein internalization, followed by 20 min incubation with 2% BSA in PBS at 4 °C. Then cells were incubated for 1 h with EphA7-Fc (1 μg ml^{-1}) at 4 °C. Cells were washed three times with cold PBS and fixed in 4% PFA/ 0.33 M sucrose for 10 min at 4 °C followed by another three washes with PBS and 10 min incubation with 2% BSA/PBS. Subsequently, cells were incubated for 1 h at 20 °C with tetramethylrhodamine isothiocyanate (TRITC)–conjugated anti-human Fc. For RGC immunocytochemistry, cells cultured for 36–48 h were fixed in 4% PFA/0.33% methylcellulose and were blocked in 2% BSA/PBS for 90 min. After washing with PBS, cells were incubated for 1 h at 20 °C with TRITC conjugated anti-human Fc.

Quantitative FRET measurements in cells. FRET was carried out as previously described[28]. The measurements were performed using a Zeiss 510 Meta confocal laser scanning microscope with a Plan-Apochromat 63 × 1.4 oil immersion objective lens. All measurements were carried out using two in-built photomultipliers. For neurons transfected with both CFP- and YFP- labeled constructs, dual excitation with 405 nm blue diode and 514 nm argon ion laser (beam splitter in front of the lasers, HFT 405/514) was used. The common beam splitter for both detectors was the NFT 490. The detectors were equipped with the band passes 420–480 nm (channel l, CFP) and 530–600 (channel 2, YFP). Pinholes were closed to 1 Airy unit. The pixel dwell time was 1.28 μs. For photobleaching measurements, two frames were recorded (both channels 1 and 2) using different excitation wavelengths (the first frame of images was recorded with only 514 nm excitation, and the second used 405 nm excitation alone). These measurements were repeated ten times in total. After the second repetition, the photobleaching light (514 nm) was employed at full power for 200 cycles on three different regions of interest (each spanning 40 × 40 pixel squares; pixel dwell time = 1.28 μs). Crosstalk of YFP in channel 1 under donor excitation was found to be negligible by measuring cells transfected with empty YFP vector. Retinal ganglion cell axons and their growth cones were selected based on their very long processes compared with that of other cell types. FRET efficiencies by acceptor photobleaching were estimated according to the following equation[28]:

$$E_{\text{bleach}} = 1 - \frac{I_{\text{Don,before}}}{I_{\text{Don,after}}}$$

where $I_{\text{Don,before}}$ represents donor intensity when all acceptors are intact prior to photobleaching, and $I_{\text{Don,after}}$ represents total donor intensity after acceptors are completely photobleached (corresponding to I_{noFRET} above). Image processing was done with the software Matlab 7 (Mathworks) and image processing toolbox Dipimage (Quantitative Imaging Group, Technical University of Delft).

Note: Supplementary information is available on the Nature Neuroscience website.

ACKNOWLEDGMENTS

We thank V. Sundaresan (King's College, London) for providing Robo2-MYC and A. Ullrich (Max-Plank-Institut for Biochemistry, Munich) for the PDGF-R vector; S. Kümper and A. Snedden for cloning Eph and ephrin constructs; and C. Jarvis, P. Gordon-Weeks, and R. Drescher for critical reading of the manuscript. This work was supported by the Wellcome Trust. R. Carvalho is a student of the Gulbenkian PhD Program in Biomedicine, Portugal. M. Beutler was supported by Deutsche Forschungs Gemeinschaft (HE 3492/2-1), Schwerpunktprogram (SPP)1128 & Higher Education Funding Council England (HEFCE). T. Ng is supported by an endowment fund from the Richard Dimbleby Cancer Fund to King's College London.

COMPETING INTERESTS STATEMENT

The authors declare that they have no competing financial interests.

Published online at http://www.nature.com/natureneuroscience/
Reprints and permissions information is available online at
http://npg.nature.com/reprintsandpermissions/

1. McLaughlin, T. & O'Leary, D.D. Molecular gradients and development of retinotopic maps. *Annu. Rev. Neurosci.* **28**, 327–355 (2005).
2. Klein, R. Eph/ephrin signaling in morphogenesis, neural development and plasticity. *Curr. Opin. Cell Biol.* **16**, 580–589 (2004).
3. Poliakov, A., Cotrina, M. & Wilkinson, D.G. Diverse roles of eph receptors and ephrins in the regulation of cell migration and tissue assembly. *Dev. Cell* **7**, 465–480 (2004).
4. Pasquale, E.B. Eph-ephrin promiscuity is now crystal clear. *Nat. Neurosci.* **7**, 417–418 (2004).
5. Kullander, K. & Klein, R. Mechanisms and functions of eph and ephrin signalling. *Nat. Rev. Mol. Cell Biol.* **3**, 475–486 (2002).
6. Knöll, B. & Drescher, U. Ephrin-As as receptors in topographic projections. *Trends Neurosci.* **25**, 145–149 (2002).
7. McLaughlin, T., Hindges, R. & O'Leary, D.D. Regulation of axial patterning of the retina and its topographic mapping in the brain. *Curr. Opin. Neurobiol.* **13**, 57–69 (2003).
8. Rashid, T. *et al.* Opposing gradients of Ephrin-As and EphA7 in the superior colliculus are essential for topographic mapping in the mammalian visual system. *Neuron* **47**, 57–69 (2005).
9. Yates, P.A., Roskies, A.L., McLaughlin, T. & O'Leary, D.D. Topographic-specific axon branching controlled by ephrin-as is the critical event in retinotectal map development. *J. Neurosci.* **21**, 8548–8563 (2001).
10. Yates, P.A., Holub, A.D., McLaughlin, T., Sejnowski, T.J. & O'Leary, D.D. Computational modeling of retinotopic map development to define contributions of EphA-ephrinA gradients, axon-axon interactions, and patterned activity. *J. Neurobiol.* **59**, 95–113 (2004).
11. Hornberger, M.R. *et al.* Modulation of EphA receptor function by coexpressed ephrinA ligands on retinal ganglion cell axons. *Neuron* **22**, 731–742 (1999).
12. Feldheim, D.A. *et al.* Topographic guidance labels in a sensory map to the forebrain. *Neuron* **21**, 1303–1313 (1998).
13. Erskine, L. *et al.* Retinal ganglion cell axon guidance in the mouse optic chiasm: expression and function of robos and slits. *J. Neurosci.* **20**, 4975–4982 (2000).
14. Niclou, S.P., Jia, L. & Raper, J.A. Slit2 is a repellent for retinal ganglion cell axons. *J. Neurosci.* **20**, 4962–4974 (2000).
15. Ringstedt, T. *et al.* Slit inhibition of retinal axon growth and its role in retinal axon pathfinding and innervation patterns in the diencephalon. *J. Neurosci.* **20**, 4983–4991 (2000).
16. Varela-Echavarria, A., Tucker, A., Puschel, A.W. & Guthrie, S. Motor axon subpopulations respond differentially to the chemorepellents netrin-1 and semaphorin D. *Neuron* **18**, 193–207 (1997).
17. Chen, H., Chedotal, A., He, Z., Goodman, C.S. & Tessier-Lavigne, M. Neuropilin-2, a novel member of the neuropilin family, is a high affinity receptor for the semaphorins Sema E and Sema IV but not Sema III. *Neuron* **19**, 547–559 (1997).
18. Labrador, J.P., Brambilla, R. & Klein, R. The N-terminal globular domain of Eph receptors is sufficient for ligand binding and receptor signaling. *EMBO J.* **16**, 3889–3897 (1997).
19. Sobieszczuk, D.F. & Wilkinson, D.G. Masking of Eph receptors and ephrins. *Curr. Biol.* **9**, R469–R470 (1999).
20. Miao, H. *et al.* Activation of EphA receptor tyrosine kinase inhibits the Ras/MAPK pathway. *Nat. Cell Biol.* **3**, 527–530 (2001).
21. Himanen, J.P. & Nikolov, D.B. Eph signaling: a structural view. *Trends Neurosci.* **26**, 46–51 (2003).
22. Himanen, J.P. *et al.* Repelling class discrimination: ephrin-A5 binds to and activates EphB2 receptor signaling. *Nat. Neurosci.* **7**, 501–509 (2004).
23. Ciossek, T., Lerch, M.M. & Ullrich, A. Cloning, characterization, and differential expression of MDK2 and MDK5, two novel receptor tyrosine kinases of the eck/eph family. *Oncogene* **11**, 2085–2095 (1995).
24. Scatchard, G. The attractions of protein for small molecules and ions *Ann. NY. Acad. Sci.* **51**, 660–672 (1949).
25. Marston, D.J., Dickinson, S. & Nobes, C.D. Rac-dependent trans-endocytosis of ephrinBs regulates Eph-ephrin contact repulsion. *Nat. Cell Biol.* **5**, 879–888 (2003).
26. Zimmer, M., Palmer, A., Kohler, J. & Klein, R. EphB-ephrinB bi-directional endocytosis terminates adhesion allowing contact mediated repulsion. *Nat. Cell Biol.* **5**, 869–878 (2003).
27. Soond, S.M., Everson, B., Riches, D.W. & Murphy, G. ERK-mediated phosphorylation of Thr735 in TNFalpha-converting enzyme and its potential role in TACE protein trafficking. *J. Cell Sci.* **118**, 2371–2380 (2005).
28. Bastiaens, P.I. & Jovin, T.M. Fluorescence resonance energy transfer microscopy. in *Cell Biology: A Laboratory Handbook* (ed. Celis, J.E.) 136–146 (Academic Press, New York, 1998).
29. Ehehalt, R., Keller, P., Haass, C., Thiele, C. & Simons, K. Amyloidogenic processing of the Alzheimer beta-amyloid precursor protein depends on lipid rafts. *J. Cell Biol.* **160**, 113–123 (2003).
30. Wu, C., Butz, S., Ying, Y. & Anderson, R.G. Tyrosine kinase receptors concentrated in caveolae-like domains from neuronal plasma membrane. *J. Biol. Chem.* **272**, 3554–3559 (1997).
31. Foster, L.J., De Hoog, C.L. & Mann, M. Unbiased quantitative proteomics of lipid rafts reveals high specificity for signaling factors. *Proc. Natl. Acad. Sci. USA* **100**, 5813–5818 (2003).
32. Yin, Y. *et al.* EphA receptor tyrosine kinases interact with co-expressed ephrin-A ligands in cis. *Neurosci. Res.* **48**, 285–296 (2004).
33. Gu, C. *et al.* The EphA8 receptor induces sustained MAP kinase activation to promote neurite outgrowth in neuronal cells. *Oncogene* **24**, 4243–4256 (2005).
34. Böhme, B. *et al.* Cell-cell adhesion mediated by binding of membrane-anchored ligand LERK-2 to the EPH-related receptor human embryonal kinase 2 promotes tyrosine kinase activity. *J. Biol. Chem.* **271**, 24747–24752 (1996).
35. Dravis, C. *et al.* Bidirectional signaling mediated by ephrin-B2 and EphB2 controls urorectal development. *Dev. Biol.* **271**, 272–290 (2004).

36. Holmberg, J., Clarke, D.L. & Frisen, J. Regulation of repulsion versus adhesion by different splice forms of an Eph receptor. *Nature* **408**, 203–206 (2000).
37. Marquardt, T. *et al.* Coexpressed EphA receptors and ephrin-A ligands mediate opposing actions on growth cone navigation from distinct membrane domains. *Cell* **121**, 127–139 (2005).
38. Davy, A. *et al.* Compartmentalized signaling by GPI-anchored ephrinA5 requires the fyn tyrosine kinase to regulate cellular adhesion. *Gen. Dev.* **13**, 3125–3135 (1999).
39. Paratcha, G. *et al.* Released GFRalpha1 potentiates downstream signaling, neuronal survival, and differentiation via a novel mechanism of recruitment of c-Ret to lipid rafts. *Neuron* **29**, 171–184 (2001).
40. Egea, J. *et al.* Regulation of EphA 4 kinase activity is required for a subset of axon guidance decisions suggesting a key role for receptor clustering in Eph function. *Neuron* **47**, 515–528 (2005).
41. Reber, M., Burrola, P. & Lemke, G. A relative signalling model for the formation of a topographic neural map. *Nature* **431**, 847–853 (2004).
42. Goodhill, G.J., Gu, M. & Urbach, J.S. Predicting axonal response to molecular gradients with a computational model of filopodial dynamics. *Neural Comput.* **16**, 2221–2243 (2004).
43. Loschinger, J., Weth, F. & Bonhoeffer, F. Reading of concentration gradients by axonal growth cones. *Phil. Trans. R. Soc. Lond. B* **355**, 971–982 (2000).
44. Drescher, U. *et al. In vitro* guidance of retinal ganglion cell axons by RAGS, a 25 kDa tectal protein related to ligands for Eph receptor tyrosine kinases. *Cell* **82**, 359–370 (1995).
45. Connor, R.J., Menzel, P. & Pasquale, E.B. Expression and tyrosine phosphorylation of Eph receptors suggest multiple mechanisms in patterning of the visual system. *Dev. Biol.* **193**, 21–35 (1998).
46. Burack, M.A., Silverman, M.A. & Banker, G. The role of selective transport in neuronal protein sorting. *Neuron* **26**, 465–472 (2000).
47. Monschau, B. *et al.* Shared and distinct functions of RAGS and ELF-1 in guiding retinal axons. *EMBO J.* **16**, 1258–1267 (1997).
48. Toth, J. *et al.* Crystal structure of an ephrin ectodomain. *Dev. Cell* **1**, 83–92 (2001).
49. Himanen, J.P. & Nikolov, D.B. Purification, crystallization and preliminary characterization of an Eph-B2/ephrin-B2 complex. *Acta Crystallogr. D Biol. Crystallogr.* **58**, 533–535 (2002).
50. Hansen, M.J., Dallal, G.E. & Flanagan, J.G. Retinal axon response to ephrinAs shows a graded, concentration-dependent transition from growth promotion to inhibition. *Neuron* **42**, 717–730 (2004).